Research Square

Preprints are preliminary reports that have not undergone peer review.
They should not be considered conclusive, used to inform clinical practice,
or referenced by the media as validated information.

Distribution-Based Residual Monitoring for Fault Detection in Chemical and Wastewater Systems

K. Ramakrishna Kini
Manipal Academy of Higher Education
Fouzi Harrou
King Abdullah University of Science and Technology
Muddu Madakyaru
muddu.m@manipal.edu

Manipal Academy of Higher Education
Ying Sun
King Abdullah University of Science and Technology

Article

Keywords:

Posted Date: June 24th, 2026

DOI: https://doi.org/10.21203/rs.3.rs-9820555/v1

License: This work is licensed under a Creative Commons Attribution 4.0 International License.
Read Full License

Additional Declarations: No competing interests reported.

Distribution-Based Residual Monitoring for Fault Detection in Chemical and Wastewater Systems

K. Ramakrishna Kini[1], Fouzi Harrou[2,*], Muddu Madakyaru[1,*], and Ying Sun[2]

[1]Manipal Institute of Technology, Manipal Academy of Higher Education, Manipal, India
[2]King Abdullah University of Science and Technology (KAUST), Computer, Electrical and Mathematical Sciences and Engineering (CEMSE) Division, Thuwal 23955-6900, Saudi Arabia
[*]muddu.m@manipal.edu; fouzi.harrou@kaust.edu.sa

ABSTRACT

Reliable fault detection is essential to ensure the safety, efficiency and sustainability of modern industrial and environmental processes. This paper presents a distribution-based residual monitoring framework for fault detection in multivariate processes. This paper proposes a Canonical Correlation Analysis (CCA)-based fault detection framework enhanced with distribution-based residual monitoring using Hellinger Distance (HD), Kullback–Leibler Distance (KLD), and Kantorovich Distance (KD). The proposed approach evaluates residual distributions within a moving-window scheme and determines detection thresholds nonparametrically using kernel density estimation (KDE), thereby avoiding restrictive Gaussian assumptions. A key advantage of the method is that it requires only fault-free data for training, making it suitable for practical applications where labeled fault data are scarce. The effectiveness of the proposed framework is demonstrated through two benchmark processes: the Williams–Otto reactor benchmark and a wastewater treatment plant process. Several representative fault scenarios, including bias, intermittent, drift, and freezing faults, are investigated. Experimental results show that distribution-based indicators significantly improve detection performance compared with conventional CCA monitoring. Among the tested indicators, the KD-based approach consistently achieves the best results, with average fault detection rates exceeding 95% and false alarm rates close to zero across the considered scenarios. Overall, the results demonstrate that integrating CCA modeling with distribution-based residual analysis provides an effective framework for monitoring in multivariate processes.

1 Introduction

Fault detection plays a critical role in ensuring the safety, reliability, and efficiency of modern industrial and environmental processes. Undetected faults may lead to degraded product quality, increased operational costs, equipment damage, and environmental or safety risks[1]. For example, small deviations in operating conditions of chemical reactors can propagate and result in off-spec products or unstable operation, while faults in wastewater treatment plants, such as sensor drift, aeration malfunction, or abnormal influent loading, can reduce treatment efficiency and increase energy consumption. These challenges are amplified by complex multivariate interactions, nonlinear dynamics, and measurement noise, which make early detection of weak or slowly developing faults difficult[2]. Recent surveys confirm that data-driven and multivariate monitoring methods remain essential for handling high-dimensional, non-Gaussian industrial data, and that improving sensitivity to incipient faults remains a hot research topic[3–5].

Over the past decades, statistical process monitoring techniques have been widely used for fault detection in industrial systems. Early approaches were mainly based on univariate control charts and sequential detection methods such as the cumulative sum (CUSUM)[6], exponentially weighted moving average (EWMA)[7], and generalized likelihood ratio (GLR) tests[8], which are effective for detecting shifts in individual process variables. However, modern industrial processes are inherently multivariate, involving large numbers of strongly correlated measurements. Monitoring each variable independently neglects cross-correlations and interactions between variables, which may lead to increased false alarm rates or missed detections, particularly when faults manifest as small but coordinated changes across multiple variables. To address these limitations, multivariate statistical process monitoring (MSPM) techniques have been developed and widely adopted. Classical MSPM approaches such as Principal Component Analysis (PCA) and Partial Least Squares (PLS) rely on monitoring statistics such as Hotelling's T^2 and the Squared Prediction Error (SPE)[9–11]. Although these methods are effective in many applications, they typically rely on Gaussian assumptions and second-order statistics, which may limit their sensitivity to subtle or distributional changes in process behavior. In many real-world processes, residuals often exhibit non-Gaussian characteristics, time-varying distributions, and weak or gradual faults that are difficult to detect using conventional monitoring indices alone[12,13].

Canonical Correlation Analysis (CCA) has emerged as an effective latent-variable modeling technique for process mon-

itoring, as it captures the correlation structure between two sets of process variables and provides meaningful residual representations. However, most CCA-based monitoring approaches still rely primarily on variance-based statistics, which may not fully exploit the information contained in the residual distributions. To address these limitations, this paper proposes a distribution-based residual monitoring framework for fault detection in multivariate processes. The proposed approach combines CCA modeling with statistical distance measures to monitor changes in the residual distribution. Instead of relying solely on scalar monitoring statistics, the method compares the distribution of residuals obtained from new data with a reference distribution estimated under normal operating conditions. Several distance measures, including the Hellinger Distance (HD), Kullback–Leibler Distance (KLD), and Kantorovich Distance (KD), are employed to detect subtle deviations and gradual distributional changes. A sliding-window strategy is used to enable online monitoring and real-time fault detection. The effectiveness of the proposed framework is demonstrated using two representative case studies: the Williams–Otto reactor benchmark and a wastewater treatment plant (WWTP) process. These systems present realistic challenges such as noise, process variability, and different types of faults, providing a suitable testbed for evaluating the robustness and sensitivity of the proposed approach. The main contributions of this work can be summarized as follows.

- A distribution-based monitoring framework that integrates Canonical Correlation Analysis (CCA) with statistical distance measures (HD, KLD, and KD) to detect faults through changes in residual distributions, allowing improved sensitivity to weak, gradual, and non-Gaussian faults compared with traditional variance-based indicators such as SPE.
- An online monitoring strategy based on sliding-window residual analysis, where the distribution of test residuals is continuously compared with a reference distribution obtained under normal operating conditions, enabling real-time detection of distributional shifts and correlation changes.
- A nonparametric threshold determination procedure based on Kernel Density Estimation (KDE), which avoids Gaussian assumptions and provides reliable decision limits for HD-, KLD-, and KD-based monitoring statistics, improving robustness in nonlinear and non-Gaussian processes.
- A comprehensive comparative study of multiple monitoring indicators (SPE, HD, KLD, and KD), including quantitative evaluation using standard performance metrics such as Fault Detection Rate (FDR), False Alarm Rate (FAR), Precision, Accuracy, and F1-score, together with validation on two benchmark case studies, the Williams–Otto reactor and a WWTP, demonstrating improved detection performance and robustness under multiple fault types (bias, drift, intermittent, and freezing faults) while requiring only fault-free data for training and no labeled fault data, making the approach suitable for practical industrial deployment.

The remainder of this paper is organized as follows. Section 2 reviews related work on multivariate statistical process monitoring and CCA-based fault detection. Section 3 presents the preliminaries, including Canonical Correlation Analysis and the statistical distance measures used for residual monitoring. Section 4 describes the proposed CCA-based fault detection strategy. Section 5 presents the case studies and discusses the experimental results. Finally, Section 6 concludes the paper and outlines directions for future work.

2 Related Work

Over the past decades, several techniques have been developed for multivariate statistical process monitoring, among which Principal Component Analysis (PCA) and Partial Least Squares (PLS) are the most widely used. PCA detects faults by modeling dominant process variability, while PLS captures input–output relationships for monitoring quality-related changes[14–16]. Although effective in many applications, these methods mainly rely on second-order statistics and variance-based monitoring, which may limit their sensitivity when faults primarily affect cross-correlations between groups of variables or manifest as subtle or incipient changes.

To better address these limitations, Canonical Correlation Analysis (CCA) has been introduced as an effective framework for capturing relationships between variable blocks. CCA projects two sets of variables onto latent spaces that maximize their correlation, making it well-suited for detecting faults that alter inter-variable relationships and for constructing correlation-based monitoring charts. Early evidence of the effectiveness of this framework was demonstrated through its dynamic extension, Canonical Variate Analysis (CVA). Russell et al.[17] applied CVA to the Tennessee Eastman process and showed that a residual-based CVA statistic achieved higher fault sensitivity than PCA by explicitly accounting for process dynamics, highlighting the potential of CCA-based methods for fault detection. Chen *et al.*[18] proposed one of the early CCA-based fault detection methods and demonstrated improved detection performance compared with PCA-based monitoring. Later, generalized CCA methods were developed to address non-Gaussian processes and improve robustness[19]. Distributed CCA strategies were further introduced for plant-wide monitoring to handle large-scale industrial systems[20]. Other studies explored extensions of CCA for

enhanced feature extraction and incipient fault detection, including explicit relation discovery approaches[21], canonical variate dissimilarity analysis[22], and statistical feature-based anomaly detection[23]. More recently, hybrid and deep learning-enhanced CCA methods have been proposed to improve sensitivity to nonlinear and time-varying faults. For example, deep recurrent CCA approaches have been applied to sensor drift diagnosis in HVAC systems[24], and gated recurrent unit (GRU)-based CCA frameworks have been developed for incipient fault detection in complex industrial processes[25].

Despite these advances, most existing studies primarily rely on variance-based statistics or residual magnitude monitoring. At the same time, limited attention has been given to analyzing distributional changes in CCA residuals using statistical distance measures. Monitoring residual distributions rather than only residual magnitudes can improve sensitivity to weak, gradual, and intermittent faults, particularly under non-Gaussian conditions. In this work, a CCA-based fault detection framework is developed in which residual distributions are monitored using statistical distance measures, including the Hellinger, Kullback–Leibler, and Kantorovich Distances. Detection thresholds are determined nonparametrically via kernel density estimation, thereby avoiding restrictive Gaussian assumptions. The proposed approach requires only fault-free data for training and is validated on two benchmark processes, demonstrating improved sensitivity and robustness compared with conventional SPE-based monitoring.

3 Preliminaries

This section presents the Canonical Correlation Analysis (CCA) modeling framework, along with the statistical distance measures used for fault detection: the Hellinger Distance (HD), Kullback–Leibler Distance (KLD), and Kantorovich Distance (KD).

3.1 Canonical Correlation Analysis for Fault Detection

Canonical Correlation Analysis (CCA) is a multivariate statistical technique used to identify linear relationships between two sets of variables. In process monitoring, the measured variables are typically divided into two blocks, denoted as $\mathbf{X} \in \mathbb{R}^{n\times m}$ and $\mathbf{Y} \in \mathbb{R}^{n\times p}$, where n is the number of samples and m and p represent the number of variables in each block. CCA seeks projection vectors $\mathbf{w}_x$ and $\mathbf{w}_y$ such that the linear combinations

$$u = \mathbf{X}\mathbf{w}_x, \quad v = \mathbf{Y}\mathbf{w}_y \tag{1}$$

maximize the correlation coefficient

$$\rho = \frac{\mathbf{w}_x^T \blacksquare_{XY} \mathbf{w}_y}{\sqrt{\mathbf{w}_x^T \blacksquare_{XX} \mathbf{w}_x}\sqrt{\mathbf{w}_y^T \blacksquare_{YY} \mathbf{w}_y}}, \tag{2}$$

where $\blacksquare_{XX}$, $\blacksquare_{YY}$, and $\blacksquare_{XY}$ are covariance matrices estimated from normal operating data. The resulting canonical variates capture the dominant correlations between the two variable blocks and form the basis of the monitoring model[26,27].

For fault detection, residuals are constructed to measure deviations from the learned correlation structure. Let $\mathbf{T}_x$ and $\mathbf{T}_y$ denote the canonical score matrices obtained from the training data. Under normal operating conditions, these scores exhibit strong correlation, while faults introduce discrepancies between them. A canonical residual vector can be defined as

$$\mathbf{r} = \mathbf{T}_x - \mathbf{T}_y, \tag{3}$$

which represents the portion of variability not explained by the canonical correlation model. The Squared Prediction Error (SPE) statistic is then computed as

$$SPE = \mathbf{r}^T \mathbf{r}. \tag{4}$$

3.2 CCA-Based Fault Detection

Canonical Correlation Analysis (CCA) is a multivariate statistical technique used to identify linear relationships between two sets of variables. In process monitoring, the measured variables are typically divided into two blocks, denoted as $\mathbf{X} \in \mathbb{R}^{n\times m}$ and $\mathbf{Y} \in \mathbb{R}^{n\times p}$, where n is the number of samples and m and p represent the number of variables in each block. CCA seeks projection vectors $\mathbf{w}_x$ and $\mathbf{w}_y$ such that the linear combinations

$$u = \mathbf{X}\mathbf{w}_x, \quad v = \mathbf{Y}\mathbf{w}_y, \tag{5}$$

maximize the correlation coefficient

$$\rho = \frac{\mathbf{w}_x^T \blacksquare_{XY} \mathbf{w}_y}{\sqrt{\mathbf{w}_x^T \blacksquare_{XX} \mathbf{w}_x}\sqrt{\mathbf{w}_y^T \blacksquare_{YY} \mathbf{w}_y}}, \tag{6}$$

where $\blacksquare_{XX}$, $\blacksquare_{YY}$, and $\blacksquare_{XY}$ are covariance matrices estimated from normal operating data.

The vectors u and v are called *canonical variates*. Each canonical variate represents a linear combination of the original variables in $\mathbf{X}$ and $\mathbf{Y}$, respectively. In practice, multiple pairs of canonical variates are extracted. Let $\mathbf{W}_x$ and $\mathbf{W}_y$ denote the projection matrices containing the first k canonical directions. The corresponding canonical score matrices are defined as

$$\mathbf{T}_x = \mathbf{X}\mathbf{W}_x, \quad \mathbf{T}_y = \mathbf{Y}\mathbf{W}_y, \tag{7}$$

where $\mathbf{T}_x$ and $\mathbf{T}_y$ contain the canonical variates for all samples. Thus, u and v represent a single pair of canonical variates, whereas $\mathbf{T}_x$ and $\mathbf{T}_y$ represent matrices formed by multiple canonical variates.

Figure 1 illustrates the principle of CCA for fault detection. The two variable blocks are projected into the canonical space, where the correlation between the canonical variates is maximized under normal operating conditions. Faults disturb this correlation structure, which appears as deviations in the canonical residuals.

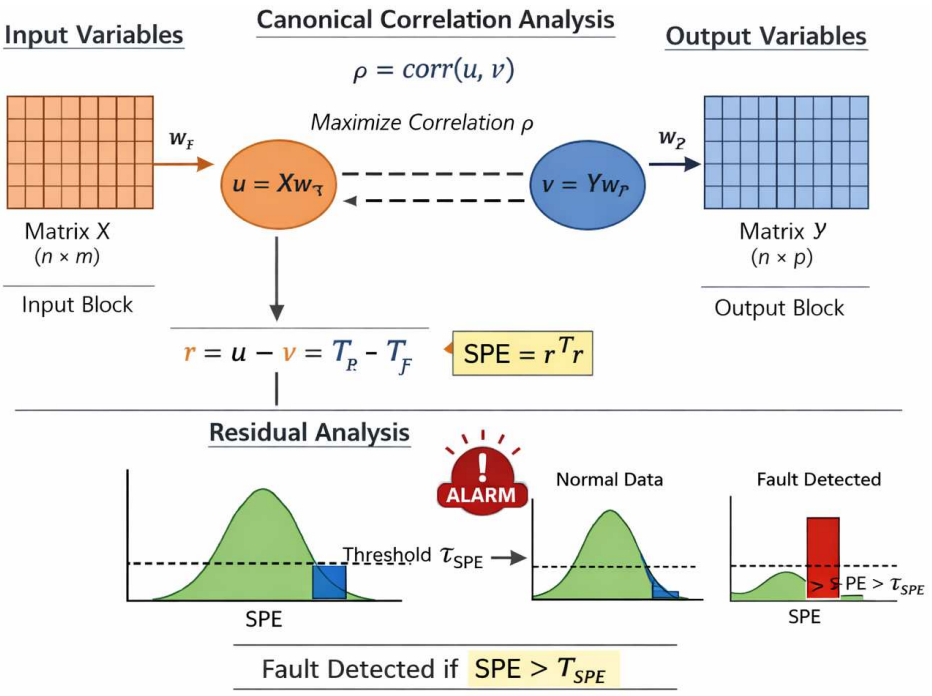


Figure 1. Conceptual illustration of Canonical Correlation Analysis (CCA) for fault detection. Process variables are divided into two blocks, projected into canonical space, and residuals are monitored to detect deviations from normal operation.

Under normal operating conditions, the canonical variates in $\mathbf{T}_x$ and $\mathbf{T}_y$ are strongly correlated, reflecting the intrinsic relationships between the two variable blocks. Faults affecting the process disturb this correlation structure, which can be detected by analyzing the canonical residuals. A residual vector can be defined as

$$\mathbf{r} = \mathbf{T}_x - \mathbf{T}_y, \tag{8}$$

which represents the portion of variability not explained by the CCA model. The Squared Prediction Error (SPE) statistic is then computed as

$$SPE = \mathbf{r}^T \mathbf{r}. \tag{9}$$

The SPE measures the magnitude of the residual and is commonly used as a monitoring index in multivariate statistical process monitoring[28]. During the training phase, SPE values are computed from normal data to determine a control limit τ_{SPE} at a specified confidence level. During online monitoring, a fault is declared when

$$SPE_t > \tau_{SPE} \tag{10}$$

indicating a significant deviation from the normal correlation structure.

CCA-based monitoring is particularly effective for detecting faults that alter relationships between variables rather than their individual variances. This makes it suitable for incipient faults and correlation-related anomalies that may not be detected by PCA-based methods[29]. However, classical CCA assumes linear relationships and approximately Gaussian residual distributions, which may limit performance under strongly nonlinear or non-Gaussian conditions, motivating extensions such as generalized and nonlinear CCA methods[27].

3.3 Statistical Distance Measures for Residual Monitoring

While the SPE statistic measures the magnitude of canonical residuals, it does not explicitly account for changes in their probability distribution, which may occur in the presence of incipient or non-Gaussian faults. To address this limitation, statistical distance measures are introduced to quantify differences between the residual distributions obtained under normal and monitoring conditions.

Statistical distance measures provide a quantitative way to compare probability distributions and detect deviations from normal operating conditions. In this work, three complementary distance measures are considered: the Hellinger Distance (HD), which measures the similarity between probability distributions; the Kullback–Leibler Distance (KLD), which quantifies the divergence between distributions from an information-theoretic perspective; and the Kantorovich Distance (KD), also known as the Wasserstein distance, which measures the optimal transport cost between distributions. These metrics enable the detection of distributional changes in residual signals and provide improved sensitivity to weak, gradual, or non-Gaussian faults.

Let P and Q denote the reference and current residual distributions, respectively, obtained from normal training data and from a monitoring window of test residuals. In practice, P and Q are estimated from residual samples (e.g., via parametric Gaussian fitting or kernel density estimation). The following distance measures are used to quantify distributional changes between P and Q.

3.3.1 Hellinger Distance (HD)

The Hellinger distance is a bounded and symmetric measure of similarity between two probability density functions $p(y)$ and $q(y)$[30–32]:

$$\begin{cases} HD^2(P,Q) = \dfrac{1}{2}\displaystyle\int \left(\sqrt{p(y)} - \sqrt{q(y)}\right)^2 dy, \\ \qquad 0 \le HD(P,Q) \le 1. \end{cases} \tag{11}$$

It is equal to zero if and only if $P = Q$. For the Gaussian case, $P = \mathcal{N}(\mu_1, \sigma_1^2)$ and $Q = \mathcal{N}(\mu_2, \sigma_2^2)$, the squared Hellinger distance admits the closed-form expression[33]:

$$HD^2(P,Q) = 1 - \sqrt{\frac{2\sigma_1\sigma_2}{\sigma_1^2+\sigma_2^2}} \exp\left(-\frac{(\mu_1-\mu_2)^2}{4(\sigma_1^2+\sigma_2^2)}\right). \tag{12}$$

If $\sigma_1 = \sigma_2 = \sigma$, this simplifies to

$$HD^2(P,Q) = 1 - \exp\left(-\frac{(\mu_1-\mu_2)^2}{8\sigma^2}\right). \tag{13}$$

HD is particularly effective in detecting small changes in the distribution because it directly measures the overlap between densities. The Hellinger distance has been widely used as a statistical measure for comparing probability distributions in various applications, including pattern recognition, classification, and anomaly detection[34–36]. It has also been applied in environmental and statistical data analysis[37] and outlier detection problems[38]. In process monitoring, HD has demonstrated strong capability for detecting nonlinear and incipient faults in chemical engineering systems, such as plug flow reactors and multivariate processes[39–42]. Owing to its sensitivity to distributional changes, the Hellinger distance is well-suited for residual-based fault detection and is therefore adopted in this work. Although HD provides a robust measure of similarity between distributions, other complementary distance measures, such as the KLD and the KD, can capture different aspects of distributional changes. These measures are therefore introduced in the following subsections to provide a more comprehensive residual monitoring framework.

3.3.2 Kullback–Leibler Distance (KLD)

The Kullback–Leibler divergence (KLD) quantifies the information loss between probability distributions and is widely used in detection, estimation, and data analysis[30,43]. Its applications span numerous fields, including pattern recognition, image processing, and classification[44–46], as well as anomaly detection and fault diagnosis in dynamic systems[47–49]. The popularity of

KLD stems from its clear probabilistic interpretation, since it corresponds to the expected log-likelihood ratio between two distributions[30,50]. These properties make KLD particularly suitable for detecting distributional changes in residual signals. The KLD quantifies the information loss when using Q to approximate P[51]:

$$KLD(P\|Q) = \int p(y) \log \frac{p(y)}{q(y)} dy. \tag{14}$$

A symmetric version is often used in monitoring:

$$KLD_s(P,Q) = \frac{1}{2}\big(KLD(P\|Q) + KLD(Q\|P)\big). \tag{15}$$

For the univariate Gaussian case, the symmetric KLD has the closed form[51]:

$$KLD_s(P,Q) = \frac{1}{2}\left(\frac{\sigma_2^2}{\sigma_1^2} + \frac{\sigma_1^2}{\sigma_2^2} + (\mu_1-\mu_2)^2\left(\frac{1}{\sigma_1^2}+\frac{1}{\sigma_2^2}\right) - 2\right). \tag{16}$$

If $\sigma_1^2 = \sigma_2^2 = \sigma^2$, it reduces to

$$KLD_s(P,Q) = \frac{(\mu_1-\mu_2)^2}{\sigma^2}. \tag{17}$$

KLD is sensitive to relative entropy changes and can capture deviations that may not produce large residual energy.

3.3.3 Kantorovich Distance (KD)

The Kantorovich distance (KD), also known as the Wasserstein distance, is an optimal transport–based measure that quantifies the minimum cost required to transform one probability distribution into another[52,53]. Unlike divergences such as KLD or HD, KD has a geometric interpretation and is sensitive to differences in distribution location, dispersion, and shape, leading to increased use in fault and anomaly detection applications[54].

It has been successfully applied to change-point detection in industrial processes, pipeline leak detection, and multivariate chemical process monitoring[55]. Recent studies have also demonstrated its effectiveness in dynamic and nonlinear systems, including sensor attack detection and representation-learning-based monitoring frameworks[53,56]. In addition, KD-based strategies have shown promising performance in energy and environmental systems, such as wastewater treatment plants and photovoltaic systems, where distributional shifts in residual signals are indicative of abnormal operating conditions[16,55]. These characteristics make KD a suitable complementary measure for monitoring residual distributions in fault detection. The Kantorovich distance, also known as the Wasserstein distance, measures the minimum cost required to transport probability mass from one distribution to another[57]:

$$KD(P,Q) = \inf_{\gamma \in \Gamma(P,Q)} \int \|y_1 - y_2\| \, d\gamma(y_1, y_2), \tag{18}$$

where $\Gamma(P,Q)$ is the set of joint distributions with marginals P and Q. For the one-dimensional Gaussian case, the 2-Wasserstein distance admits a closed form[57]:

$$W_2^2(P,Q) = (\mu_1-\mu_2)^2 + (\sigma_1-\sigma_2)^2. \tag{19}$$

KD has a geometric interpretation and is effective for detecting shifts in distribution location and shape.

In summary, HD emphasizes distribution overlap, KLD measures relative entropy, and KD captures transport-based geometric shifts. Their combined use provides a comprehensive characterization of residual distribution changes and improves sensitivity to weak, gradual, and non-Gaussian faults. The main characteristics and practical considerations of these distance measures are summarized in Table 1.

In online monitoring, residual samples are continuously collected and analyzed using a sliding window approach. At each time instant, a window of recent residuals is used to estimate the current residual distribution, which is then compared with the reference distribution obtained during normal operation. Statistical distance measures such as HD, KLD, or KD are computed between the two distributions, and a fault alarm is triggered when the distance exceeds a predefined threshold. This approach enables the detection of gradual or distributional changes that may not be captured by variance-based statistics alone. Figure 2 illustrates the principle of distance-based distribution monitoring using a moving window.

Table 1. Comparison of distance-based indicators used for anomaly detection

Property	Hellinger Distance (HD)	Kullback-Leibler Distance(KLD)	Kantorovich Distance (KD)
Type of Measure	Statistical distance	Information divergence	Optimal transport distance
Symmetry	Yes	No (Yes if symmetrized)	Yes
Metric Properties	True metric	Not a metric	True metric
Range	Bounded (0 to 1)	Unbounded	Unbounded
Sensitivity	Sensitive to small distribution changes	Sensitive to tail differences	Sensitive to shape and location shifts
Interpretation	Overlap between distributions	Information loss between distributions	Minimum transport cost between distributions
Robustness to Noise	Moderate to high	Sensitive to estimation errors	High robustness
Distribution Assumptions	None (can use KDE)	Requires density estimation	None (works well with empirical distributions)
Computational Cost	Low	Low	Moderate to high
Suitability for Fault Detection	Good for detecting small deviations	Effective for mean/variance changes	Effective for drift and distribution shifts

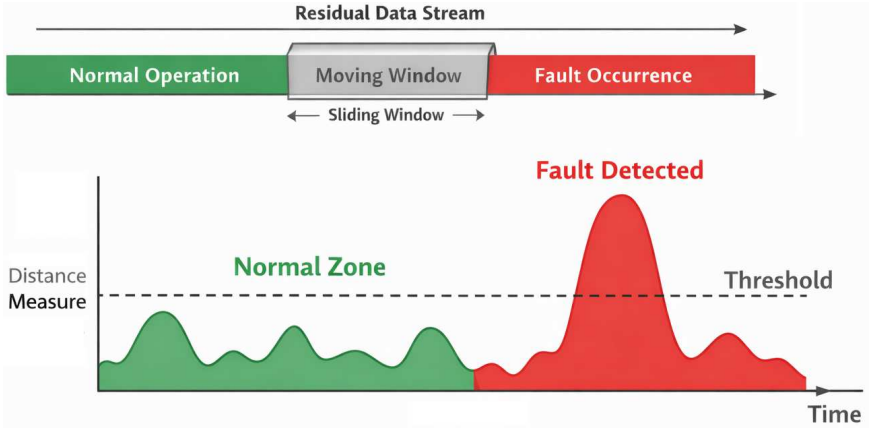


Figure 2. Illustration of distance-based distribution monitoring for fault detection using a sliding window approach. A reference residual distribution is compared with the distribution estimated from a moving window of recent data. Faults are detected when the computed statistical distance exceeds the decision threshold.

4 Proposed CCA-Based Fault Detection Strategy

This section presents the proposed Canonical Correlation Analysis (CCA)-based fault detection strategy. The approach combines latent-variable modeling with distribution-based residual monitoring to detect abnormal operating conditions in multivariate processes. Residuals generated from the CCA model are evaluated using several statistical indicators, including the Squared Prediction Error (SPE), Hellinger Distance (HD), Kullback–Leibler Distance (KLD), and Kantorovich Distance (KD). This combination enables the detection of both energy-based deviations and subtle distributional changes in residual signals.

The overall framework of the proposed method is illustrated in Fig. 3. The procedure consists of two main stages: a training phase performed under normal operating conditions and an online monitoring phase applied to newly acquired process data.

During the training phase, normal operating data are used to build the CCA model, which captures the correlation structure between process variables. The corresponding training residuals are then used to estimate a reference residual distribution representing normal system behavior. Based on this reference distribution, decision thresholds are determined for the monitoring statistics, including SPE and the distribution-based measures HD, KLD, and KD. During the monitoring phase, newly acquired process data are projected onto the trained CCA model to obtain residuals. A moving window is employed to estimate the residual distribution in real time, which is continuously compared with the reference distribution obtained during training. A fault alarm is triggered when any monitoring statistic exceeds its predefined threshold; otherwise, the process is considered to operate under normal conditions.

[!htbp] KwInInput KwOutOutput

Normal training data $\mathscr{D}_{tr} = \{(\mathbf{x}(i), \mathbf{y}(i))\}_{i=1}^{N_{tr}}$; test data stream $\mathscr{D}_{te} = \{(\mathbf{x}(t), \mathbf{y}(t))\}_{t=1}^{N_{te}}$; number of canonical components k; window length W; kernel $K(\cdot)$ and bandwidth h (for KDE thresholding); significance level α. Alarm flag $A_t \in \{0,1\}$ and monitoring statistics $SPE_t, D_t^{HD}, D_t^{KLD}, D_t^{KD}$.

Training Phase (Normal Operation Only) **1)** Standardize training data and fit CCA Compute mean/variance from $\mathscr{D}_{tr}$ and standardize $\mathbf{X}_{tr}, \mathbf{Y}_{tr}$. Estimate CCA projection matrices $\mathbf{W}_x, \mathbf{W}_y$ (retain k components).

2) Compute training residuals and SPE Compute canonical scores $\mathbf{T}_{x,tr} = \mathbf{X}_{tr}\mathbf{W}_x$ and $\mathbf{T}_{y,tr} = \mathbf{Y}_{tr}\mathbf{W}_y$. Compute canonical residuals $\mathbf{r}_{tr}(i) = \mathbf{t}_{x,tr}(i) - \mathbf{t}_{y,tr}(i)$. Compute $SPE_{tr}(i) = \mathbf{r}_{tr}(i)^\top \mathbf{r}_{tr}(i)$ for $i = 1, \ldots, N_{tr}$.

3) Build reference residual distribution Estimate reference residual distribution P_{ref} from $\{\mathbf{r}_{tr}(i)\}_{i=1}^{N_{tr}}$ (Gaussian fit or KDE).

4) Determine thresholds Set $\tau_{SPE} \leftarrow \text{Quantile}_{1-\alpha}\big(\{SPE_{tr}(i)\}\big)$. Using a moving window of size W on $\{\mathbf{r}_{tr}(i)\}$, compute distance sequences $\{D_{tr}^{HD}(j)\}$, $\{D_{tr}^{KLD}(j)\}$, $\{D_{tr}^{KD}(j)\}$ between P_{ref} and window distributions. Estimate their densities with KDE and set thresholds $\tau_{HD}, \tau_{KLD}, \tau_{KD}$ as the $(1-\alpha)$-percentiles.

Online Monitoring Phase (New Data) Initialize an empty buffer $\mathscr{B} \leftarrow \emptyset$. $t = 1$ N_{te} **5)** Standardize and project new sample Standardize $(\mathbf{x}(t), \mathbf{y}(t))$ using training mean/variance. Compute scores $\mathbf{t}_x(t) = \mathbf{x}(t)^\top \mathbf{W}_x$ and $\mathbf{t}_y(t) = \mathbf{y}(t)^\top \mathbf{W}_y$. Compute residual $\mathbf{r}(t) = \mathbf{t}_x(t) - \mathbf{t}_y(t)$ and $SPE_t = \mathbf{r}(t)^\top \mathbf{r}(t)$.

6) Update sliding window Append $\mathbf{r}(t)$ to buffer $\mathscr{B}$; if $|\mathscr{B}| > W$, remove the oldest residual.

7) Compute distribution distances (when window is full) $|\mathscr{B}| = W$ Estimate window residual distribution P_t from $\mathscr{B}$. Compute $D_t^{HD} = HD(P_{ref}, P_t)$, $D_t^{KLD} = KLD(P_{ref} \| P_t)$ (or symmetric KLD), and $D_t^{KD} = KD(P_{ref}, P_t)$. Set $D_t^{HD} = 0$, $D_t^{KLD} = 0$, $D_t^{KD} = 0$ *insufficient samples

8) Decision rule $A_t \leftarrow \mathbb{I}\big((SPE_t > \tau_{SPE}) \vee (D_t^{HD} > \tau_{HD}) \vee (D_t^{KLD} > \tau_{KLD}) \vee (D_t^{KD} > \tau_{KD})\big)$.

The detailed steps of the proposed monitoring procedure are summarized in Algorithm 4. The algorithm describes the training stage, reference distribution estimation, threshold computation, and real-time monitoring using sliding-window residual analysis and distance-based indicators.

For the distribution-based fault indicators, detection thresholds are determined using kernel density estimation (KDE). KDE provides a flexible and nonparametric estimate of the probability density function of monitoring statistics under normal operating conditions, without assuming a specific parametric form. This is particularly suitable for chemical and wastewater processes, where residuals and monitoring statistics may exhibit non-Gaussian behavior due to nonlinear dynamics and external disturbances.

Mathematically, given a set of fault-free statistics $\{y_1, y_2, \ldots, y_d\}$, the KDE estimate of the probability density function is expressed as

$$\hat{f}(y) = \frac{1}{dh} \sum_{i=1}^{d} K\left(\frac{y - y_i}{h}\right), \tag{20}$$

where $\hat{f}(y)$ denotes the estimated density, $K(\cdot)$ is the kernel function (typically Gaussian), and h is the bandwidth parameter controlling the smoothness of the estimate. The detection threshold is then selected as a high percentile (e.g., 95% or 99%) of the estimated distribution, ensuring a controlled false alarm rate while maintaining sensitivity to abnormal behavior.

To quantitatively evaluate the performance of the proposed fault detection strategy, several standard performance metrics are considered, including the Fault Detection Rate (FDR), also referred to as the True Positive Rate (TPR), the False Alarm Rate (FAR), Precision, Accuracy, and the F1-score. These metrics provide complementary information regarding detection capability, reliability, and robustness of the monitoring scheme under different fault scenarios.

5 Results and Discussion

This section evaluates the performance of the proposed CCA-based fault detection strategy using two benchmark processes: the Williams–Otto reactor, a nonlinear two-step reaction system widely used to simulate realistic sensor and actuator faults, and a wastewater treatment plant. Four common sensor fault types, bias, intermittent, drift, and freezing, are considered to assess the effectiveness of the proposed method.

5.1 Application to the Williams–Otto Reactor Process

The effectiveness of the proposed monitoring approach is evaluated using the Williams–Otto reactor. This benchmark process is widely used in monitoring and control studies because of its multiple reactions and strong nonlinear dynamics[58]. The reactor involves three irreversible reactions:

$$A + B \xrightarrow{k_1} C, \qquad k_1 = 1.6599 \times 10^6 \, e^{-6666.7/T_R}$$

$$B + C \xrightarrow{k_2} P + E, \quad k_2 = 7.2117 \times 10^8 \, e^{-8333.3/T_R}$$

$$C + P \xrightarrow{k_3} G, \qquad k_3 = 2.6745 \times 10^{12} \, e^{-11111/T_R}$$

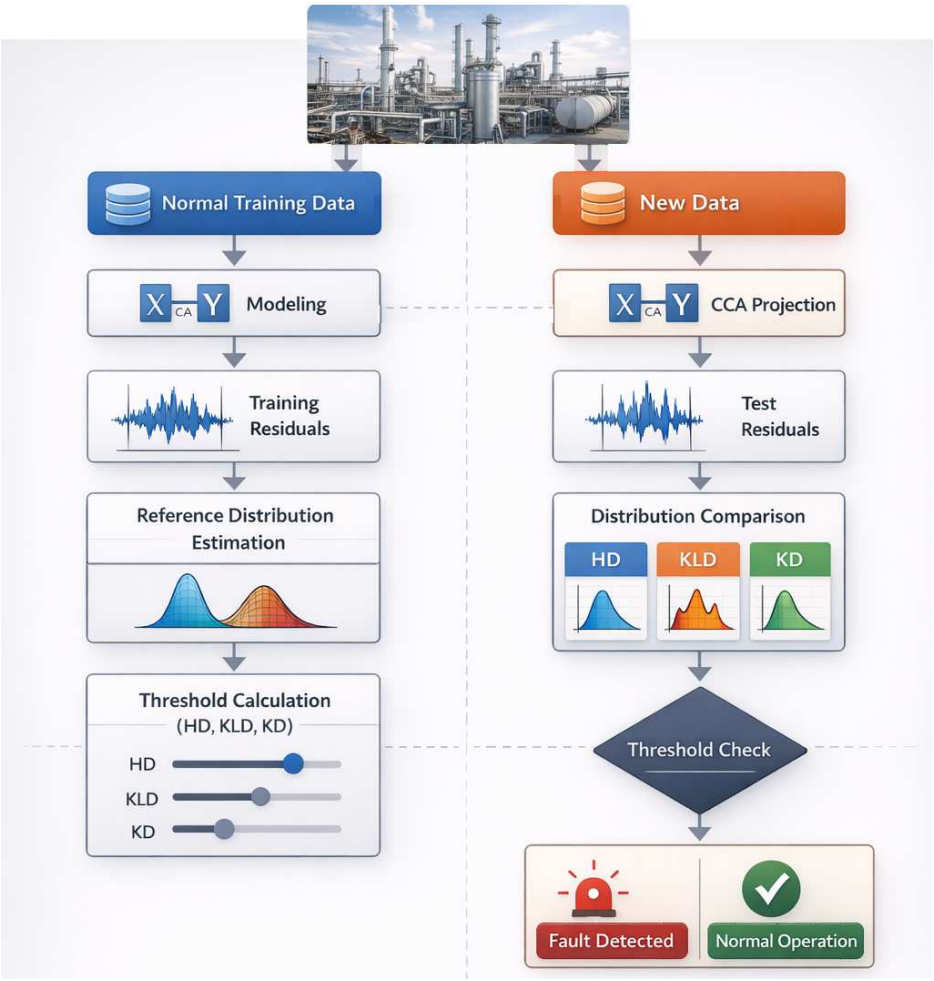


Figure 3. Block diagram of the proposed CCA-based fault detection framework. Normal operating data are used to build the CCA model and estimate a reference residual distribution. During online monitoring, new data are projected onto the trained model, residual distributions are estimated using a moving window, and statistical distance measures (HD, KLD, and KD) together with SPE are used to detect abnormal operating conditions.

The dynamic mass balances describing the reactor behavior are given by:

$$W\frac{dX_A}{dt} = F_A - (F_A + F_B)X_A - r_1 \tag{21}$$

$$W\frac{dX_B}{dt} = F_B - (F_A + F_B)X_B - r_1 - r_2 \tag{22}$$

$$W\frac{dX_C}{dt} = -(F_A + F_B)X_C + 2r_1 - 2r_2 - r_3 \tag{23}$$

$$W\frac{dX_E}{dt} = -(F_A + F_B)X_E + r_2 \tag{24}$$

$$W\frac{dX_G}{dt} = -(F_A + F_B)X_G + 1.5r_3 \tag{25}$$

$$W\frac{dX_P}{dt} = -(F_A + F_B)X_P + r_2 - 0.5r_3 \tag{26}$$

where X_A, X_B, X_C, X_E, X_G, and X_P denote the mass fractions of components A, B, C, E, G, and P, respectively, and W represents the mass of the reacting mixture. The reaction rates are defined as:

$$\begin{aligned} r_1 &= k_1 X_A X_B W, \\ r_2 &= k_2 X_B X_C W, \\ r_3 &= k_3 X_C X_P W. \end{aligned} \tag{27}$$

The state variables X_A, X_B, X_C, X_E, X_G, and X_P are considered measured outputs. The manipulated inputs are the flow rate of reactant B (F_B) and the reactor temperature (T_R), while the flow rate of reactant A (F_A) is treated as a disturbance varying around its nominal value. The mass holdup is fixed at $W = 2104.7$ kg. The open-loop simulation is performed at the nominal steady-state operating conditions given by
$X_s = [0.0875 \;\; 0.3896 \;\; 0.0153 \;\; 0.2907 \;\; 0.1075 \;\; 0.1095]^T$,
$u_s = \begin{bmatrix} 4.7836 & 89.647 \end{bmatrix}^T$.

The proposed CCA-based fault detection (FD) strategy was evaluated under four representative fault scenarios injected into the output variable X_A, namely bias, intermittent, drift, and freezing faults.

Scenario 1: Bias Fault A bias fault was introduced in the output variable X_A from time step 500 until the end of the testing period, with magnitudes of 3%, 5%, and 10% of the variable's dynamic range. The dataset consists of 2000 samples, split equally into 1000 fault-free training samples and 1000 test samples. The variable X_A was selected as the output variable in the CCA model. The reference CCA model was developed using normal data and retained four latent variables. For the distance-based indicators (HD, KLD, and KD), a 60-window moving average was used to estimate residual distributions during monitoring. Precise detection of intermittent faults is critical because their temporary appearance can cause irregular process behavior and may be overlooked by conventional monitoring methods. Table 2 summarizes the detection performance of CCA-SPE, CCA-HD, CCA-KLD, and CCA-KD for different bias magnitudes. For large faults (10%), all indicators achieved high detection performance, with F1-scores above 96%, while CCA-KD provided the best result (99.82%).

Table 2. Monitoring performance of CCA-based indicators (SPE, HD, KLD, KD) for bias fault detection in the WOR process at different magnitudes.

Magnitude	Metric	CCA-SPE	CCA-HD	CCA-KLD	CCA-KD
5*10%	FDR	92.55	94.00	92.45	99.65
	FAR	0.00	0.00	0.00	0.00
	Precision	100.0	100.0	100.0	100.0
	Accuracy	96.25	97.00	96.20	99.83
	F1-score	96.11	96.90	96.07	99.82
5*5%	FDR	72.00	92.80	87.60	98.95
	FAR	0.00	0.00	0.00	0.00
	Precision	100.0	100.0	100.0	100.0
	Accuracy	86.00	96.40	93.80	99.47
	F1-score	83.72	96.25	93.40	99.47
5*3%	FDR	58.80	88.90	61.00	97.20
	FAR	0.00	0.00	0.00	0.00
	Precision	100.0	100.0	100.0	100.0
	Accuracy	79.41	94.40	80.50	98.62
	F1-score	74.05	94.06	75.77	98.58

For medium faults (5%), the performance of CCA-SPE decreased significantly (F1-score of 83.72%), whereas CCA-HD and CCA-KLD maintained good detection accuracy. The CCA-KD indicator remained the most effective, achieving an F1-score of 99.47%.

For small faults (3%), the detection performance of SPE and KLD decreased considerably, and HD showed moderate sensitivity. In contrast, CCA-KD maintained strong detection capability, achieving an F1-score of 98.58%, demonstrating its robustness in detecting weak faults.

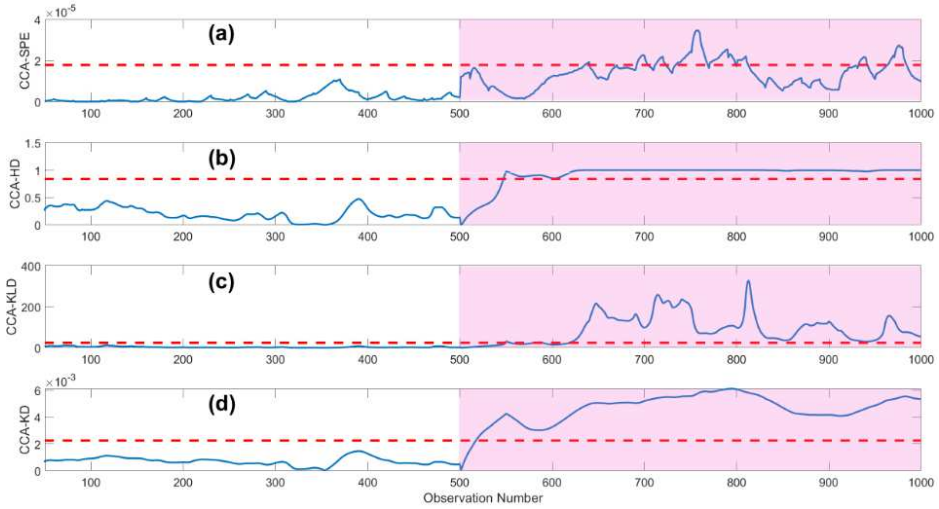


Figure 4. Bias fault monitoring in the WOR process using CCA-based indicators: (a) SPE, (b) HD, (c) KLD, and (d) KD. The red dashed line denotes the detection threshold.

Table 3. Intermittent fault detection in the WOR process using CCA-based indicators (SPE, HD, KLD, KD).

Index	CCA-SPE	CCA-HD	CCA-KLD	CCA-KD
FDR	18.65	93.33	63.55	98.45
FAR	0.00	0.00	0.00	0.00
Precision	100.00	100.00	100.00	100.00
Accuracy	75.59	97.98	89.11	99.53
F1-score	31.43	96.45	77.51	99.21

The monitoring results for the small-magnitude bias fault are illustrated in Fig. 10. As observed, CCA-SPE exhibits missed detections, while HD and KLD detect the fault with some delay. The KD-based indicator detects the fault more promptly and consistently, reflecting its higher sensitivity to small distributional changes.

Scenario 2: Intermittent Fault An intermittent fault with a magnitude of 2% was injected into the output variable X_A over two time intervals: [250, 400] and [700, 850]. Accurate detection of intermittent faults is critical because their temporary appearance can cause irregular process behavior and may be overlooked by conventional monitoring methods. Table 3 summarizes the monitoring performance of CCA-SPE, CCA-HD, CCA-KLD, and CCA-KD for this fault.

The CCA-SPE indicator shows poor detection performance, resulting in an FDR of 18.65% and an F1-score of 31.43%, indicating a high number of missed detections (Table 3). In contrast, the CCA-HD method provides strong detection performance, achieving an accuracy of 97.98% and an F1-score of 96.45%. The CCA-KLD method improves detection over SPE but still shows partial detection, yielding an F1-score of 77.51%. Among all the indicators, the CCA-KD method achieves the best performance, with an F1-score of 99.21% and an accuracy of 99.53%, demonstrating superior sensitivity to intermittent faults. These results further highlight the advantage of transport-based distance measures in detecting irregular and time-varying faults.

Scenario 3: Drift Fault A drift fault was introduced in the output variable X_A starting at time step 500, with a gradual increase characterized by a slope of 0.002. Timely detection of drift faults is essential because small but persistent deviations can accumulate over time, leading to control deterioration, increased operating costs, and potential safety risks. Figure 5 shows the time evolution of the monitoring statistics obtained using CCA-SPE, CCA-HD, CCA-KLD, and CCA-KD. All four indicators are able to detect the drift fault; however, differences in detection delay can be observed. While CCA-SPE, CCA-HD, and CCA-KLD detect the fault around time step 600, the CCA-KD indicator detects the fault earlier, at approximately time step 575, demonstrating faster sensitivity to gradual changes.

The quantitative performance comparison is summarized in Table 4. All methods provide satisfactory detection results, with F1-scores exceeding 89%. Among them, the CCA-KD method achieves the best performance, with an F1-score of 93.72% and an accuracy of 93.97%, indicating improved sensitivity and robustness in detecting slowly evolving faults.

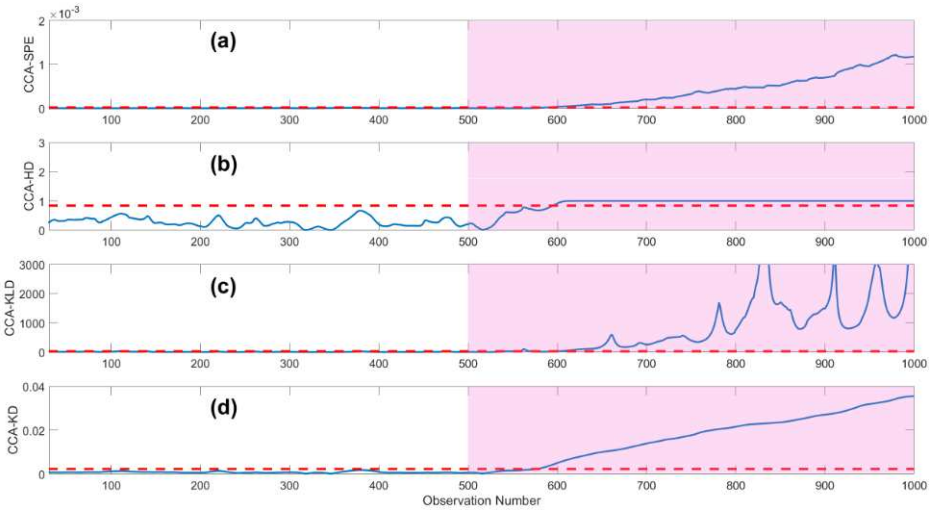


Figure 5. Freezing fault monitoring in the WOR process using CCA-based indicators: (a) SPE, (b) HD, (c) KLD, (d) KD.

Table 4. Drift fault detection in the WOR process using CCA-based indicators (SPE, HD, KLD, KD).

Index	CCA-SPE	CCA-HD	CCA-KLD	CCA-KD
FDR	80.61	81.22	83.80	87.95
FAR	0.00	0.00	0.00	0.00
Precision	100.00	100.00	100.00	100.00
Accuracy	90.31	90.61	91.90	93.97
F1-score	89.26	89.65	91.18	93.72

Scenario 4: Freezing Fault A freezing fault was introduced in the output variable X_A, where the sensor value was held constant at 0.4 starting from time step 400, simulating a frozen sensor condition. Reliable detection of freezing faults is essential to prevent incorrect control actions and to maintain process stability and product quality. Table 5 summarizes the monitoring performance of CCA-SPE, CCA-HD, CCA-KLD, and CCA-KD. All methods successfully detected the fault, achieving a fault detection rate (FDR) of 100%. However, CCA-SPE, CCA-HD, and CCA-KLD produced a small number of false alarms during normal operation, slightly reducing their overall performance. In contrast, the CCA-KD indicator achieved zero false alarms and therefore obtained the best overall performance, with 100% accuracy and F1-score. These results indicate that although freezing faults are relatively easy to detect, transport-based distance measures provide improved reliability by reducing false alarms.

5.2 Application to the BSM1 Wastewater Treatment Plant

In this section, the performance of the proposed CCA-based fault detection strategy is evaluated for monitoring sensor faults in a benchmark wastewater treatment process. The Benchmark Simulation Model No. 1 (BSM1) is considered, as it is widely used for evaluating control, monitoring, and optimization methods in wastewater treatment systems[59]. The influent data of BSM1 under dry weather conditions consists of eight key variables describing the organic and nitrogen content of wastewater, as well as the influent flow rate. Table 6 lists the symbols, definitions, and units of the considered variables.

The BSM1 treatment line comprises a five-compartment biological reactor followed by a secondary clarifier. The biological

Table 5. Freezing fault detection in the WOR process using CCA-based indicators (SPE, HD, KLD, KD).

Index	CCA-SPE	CCA-HD	CCA-KLD	CCA-KD
FDR	100.00	100.00	100.00	100.00
FAR	1.02	1.60	0.56	0.00
Precision	99.00	98.71	99.40	100.00
Accuracy	99.50	99.35	99.65	100.00
F1-score	99.48	99.35	99.70	100.00

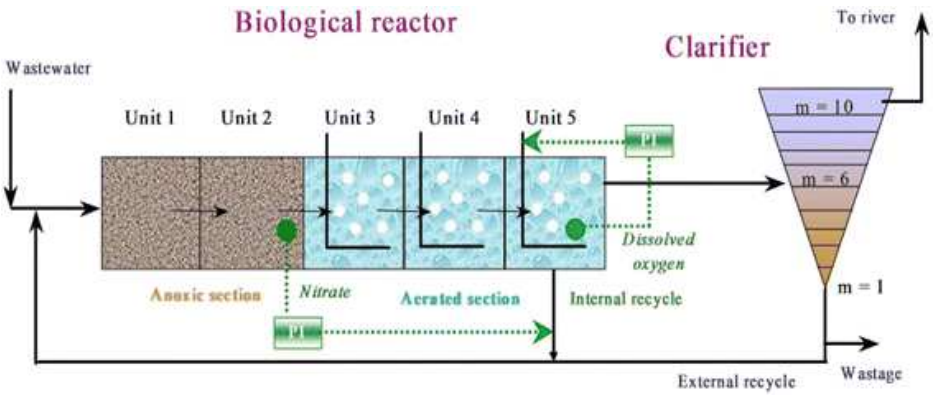


Figure 6. Schematic diagram of the BSM1 wastewater treatment process including anoxic and aerobic tanks, internal and external recirculation, and clarifier.

reactor is designed to achieve effective nitrogen removal and includes two anoxic tanks (Units 1 and 2) followed by three aerobic tanks (Units 3 to 5). The anoxic zones primarily facilitate denitrification, while the aerobic sections support both organic matter degradation and nitrification processes. The hydraulic arrangement reflects practical process configurations observed in full-scale wastewater treatment plants. The hydraulic and biological dynamics are supported by multiple flow streams. The influent enters Unit 1 (first anoxic tank), initiating the biological treatment process. Nitrate-rich mixed liquor from the last aerobic tank (Unit 5) is recycled internally to the anoxic zone to support denitrification. In parallel, an external recycle of settled sludge from the clarifier returns to the head of the reactor, maintaining sufficient biomass. Excess sludge (WAS) is removed from the system at the end of the aerobic section for solids management. The layout of BSM1 follows a left-to-right horizontal configuration, clearly showing the progression of flow and interactions between compartments. Figure 6 illustrates this configuration, including the five biological units, internal and external recirculation loops, and the clarifier that separates treated effluent and sludge.

Table 6. Considered influent variables in the BSM1 simulation

Symbol	Definition	Unit
S_S	Readily biodegradable substrate	g COD m^{-3}
X_I	Particulate inert organic matter	g COD m^{-3}
X_S	Slowly biodegradable substrate	g COD m^{-3}
$X_{B,H}$	Active heterotrophic biomass	g COD m^{-3}
S_{NH}	Ammonium + ammonia nitrogen	g N m^{-3}
S_{ND}	Soluble biodegradable organic nitrogen	g N m^{-3}
X_{ND}	Particulate biodegradable organic nitrogen	g N m^{-3}
Q_i	Influent flow to the anoxic section	m^3 d^{-1}

The proposed CCA-based fault detection (FD) strategy was evaluated under four representative fault scenarios injected into the influent flow variable Q_i in the testing dataset, namely bias, intermittent, drift, and freezing faults.

Scenario 1: Bias Fault A bias fault was introduced in the influent flow variable Q_i starting at time step 340 until the end of the testing period, with magnitudes of 1.5%, 3%, and 5% of the variable's dynamic range. Early detection of bias faults is important, as persistent offsets in flow measurements may lead to incorrect process regulation and reduced treatment efficiency. The generated dataset consists of 1340 samples, divided equally into 670 fault-free training samples and 670 testing samples. The variable Q_i was selected as the output variable in the CCA model. The reference CCA model was developed using normal data, retaining three latent variables. For the distance-based indicators (HD, KLD, and KD), a sliding window of length 50 was used to estimate residual distributions during monitoring.

Table 7 summarizes the monitoring performance of CCA-SPE, CCA-HD, CCA-KLD, and CCA-KD for different bias magnitudes. For large faults (5%), all indicators achieved good detection performance, with high accuracy and F1-scores. Among them, the CCA-KD indicator provided the best results.

For medium faults (3%), the CCA-SPE indicator showed poor detection performance, reflected in low accuracy and F1-score

Table 7. Bias fault detection in the WWT process using CCA-based indicators (SPE, HD, KLD, KD) at different magnitudes.

Magnitude	Metric	CCA-SPE	CCA-HD	CCA-KLD	CCA-KD
5*5%	FDR	86.77	95.03	92.82	98.34
	FAR	0.00	0.00	0.00	0.00
	Precision	100.0	100.0	100.0	100.0
	Accuracy	93.28	97.47	96.37	99.15
	F1-score	92.91	97.45	96.25	99.16
5*3%	FDR	37.88	91.71	88.62	96.45
	FAR	0.00	0.00	0.00	0.00
	Precision	100.0	100.0	100.0	100.0
	Accuracy	68.47	95.78	94.22	98.21
	F1-score	54.94	95.67	93.96	98.22
5*1.5%	FDR	10.79	86.79	66.78	94.64
	FAR	0.00	0.00	0.00	0.00
	Precision	100.0	100.0	100.0	100.0
	Accuracy	54.72	93.29	81.64	97.28
	F1-score	19.69	92.87	80.00	97.24

Table 8. Monitoring performance of CCA-based indicators (SPE, HD, KLD, KD) for intermittent fault detection in the WWT process.

Index	CCA-SPE	CCA-HD	CCA-KLD	CCA-KD
FDR	6.27	72.54	62.33	97.25
FAR	0.00	0.00	0.00	0.00
Precision	100.00	100.00	100.00	100.00
Accuracy	72.02	91.80	88.75	99.17
F1-score	11.79	84.08	76.79	98.59

values despite the absence of false alarms. The HD, KLD, and KD indicators demonstrated significantly improved detection, with KD achieving the best performance (accuracy of 98.21% and F1-score of 98.22%). For small faults (1.5%), the CCA-SPE method failed to detect the fault, while the HD and KLD indicators showed partial detection. In contrast, the CCA-KD indicator maintained reliable performance with high accuracy and F1-score values. The monitoring results for the small-magnitude bias fault are illustrated in Fig. 7. As observed, CCA-SPE fails to detect the fault, while HD and KLD provide improved but imperfect detection. The KD-based indicator detects the fault more consistently with minimal missed detections, demonstrating higher sensitivity to small distributional changes.

Scenario 2: Intermittent Fault An intermittent fault with a magnitude of 2% was injected into the influent flow variable Q_i over two time intervals: [125, 250] and [450, 575]. Accurate detection of intermittent faults is important, as their sporadic nature may cause irregular process behavior and can be easily overlooked by conventional monitoring methods. Figure 8 illustrates the monitoring statistics obtained using CCA-SPE, CCA-HD, CCA-KLD, and CCA-KD. The CCA-SPE indicator fails to identify the fault, while the CCA-HD and CCA-KLD methods provide partial detection with several missed detections during the fault intervals. In contrast, the CCA-KD indicator detects the fault more consistently with fewer missed detections, demonstrating improved sensitivity to intermittent disturbances.

Table 8 summarizes the quantitative performance of the four indicators. The CCA-SPE method shows poor detection capability, reflected in a low F1-score of 11.79%. The HD and KLD indicators improve detection performance but still exhibit partial detection, with F1-scores of 84.08% and 76.79%, respectively. Among all methods, the CCA-KD indicator achieves the best performance, with an F1-score of 98.59% and an accuracy of 99.17%, confirming its effectiveness in detecting intermittent faults.

Scenario 3: Drift Fault A drift fault was introduced in the influent flow variable Q_i, starting at time step 340 with a gradual increase characterized by a slope of 50. Early detection of drift faults is important, as slow deviations may accumulate over time and progressively degrade process monitoring and control performance.

Figure 9 shows the time evolution of the monitoring statistics obtained using CCA-SPE, CCA-HD, CCA-KLD, and

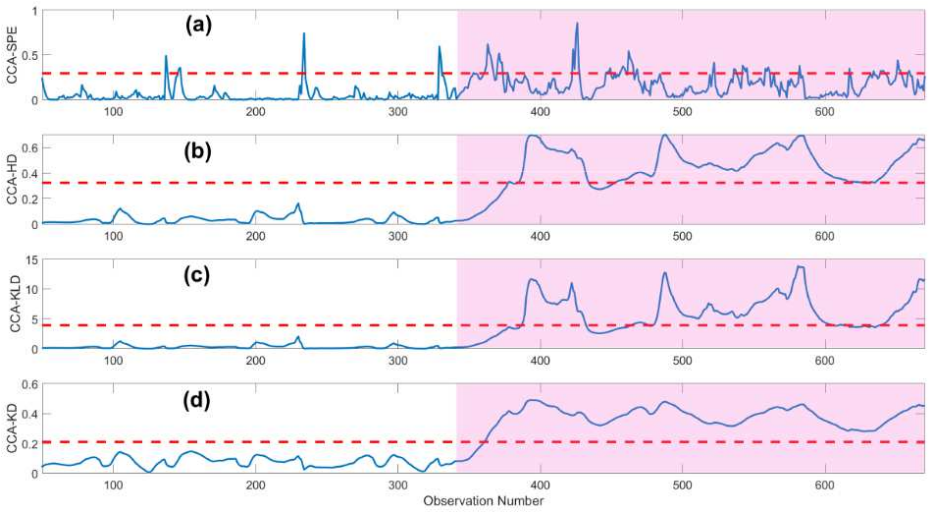


Figure 7. Monitoring of a low-magnitude bias fault (1.5% of total variation) in the WWT process using CCA-based indicators: (a) SPE, (b) HD, (c) KLD, and (d) KD. The red dashed line denotes the detection threshold.

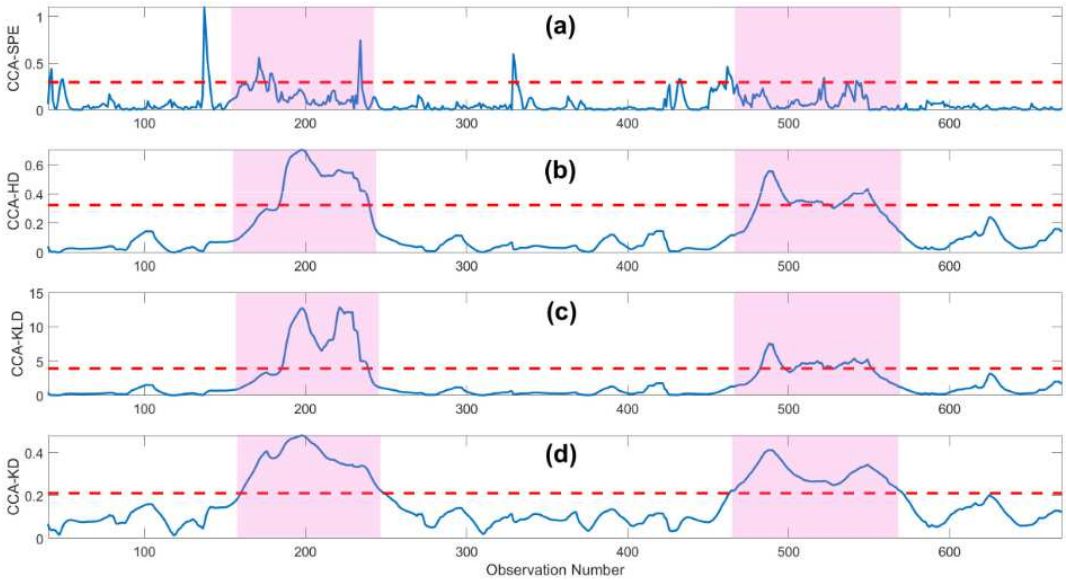


Figure 8. Intermittent fault monitoring in the WWT process using CCA-based indicators: (a) SPE, (b) HD, (c) KLD, (d) KD.

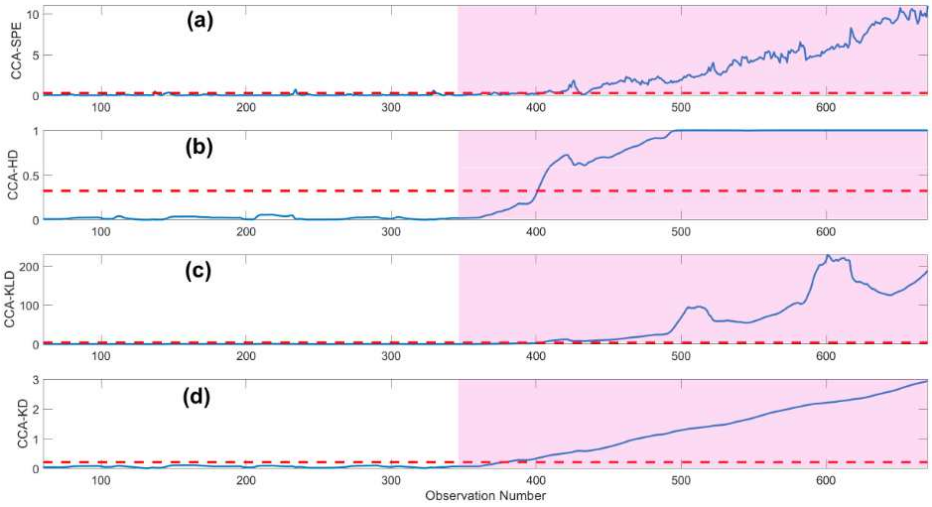


Figure 9. Monitoring of a drift fault in the WWT process using CCA-based indicators: (a) SPE, (b) HD, (c) KLD, and (d) KD. The red dashed line denotes the detection threshold.

Table 9. Drift fault detection in the WWT process using CCA-based indicators (SPE, HD, KLD, KD).

Index	CCA-SPE	CCA-HD	CCA-KLD	CCA-KD
FDR	79.09	84.84	83.94	90.30
FAR	2.05	0.00	0.00	0.00
Precision	97.38	100.00	100.00	100.00
Accuracy	89.38	92.31	91.25	95.07
F1-score	87.03	91.80	91.26	94.78

CCA-KD. All four indicators are able to detect the drift fault; however, differences in detection delay are observed. While CCA-SPE, CCA-HD, and CCA-KLD detect the fault around time step 400, the CCA-KD indicator detects the fault earlier, at approximately time step 385, demonstrating improved sensitivity to gradual changes.

Table 9 summarizes the quantitative performance of the four indicators. All methods provide satisfactory detection results, with high accuracy and F1-scores. Among them, the CCA-KD method achieves the best performance, with an accuracy of 95.07% and an F1-score of 94.78%, reflecting faster detection and improved robustness.

Scenario 4: Freezing Fault A freezing fault was introduced in the influent flow variable Q_i, where the sensor value was held constant at 6.0 starting from time step 320, simulating a frozen sensor condition. Early detection of such faults is important, as frozen measurements may mislead control decisions and degrade process performance if not promptly identified.

Figure 10 shows the time evolution of the monitoring statistics obtained using CCA-SPE, CCA-HD, CCA-KLD, and CCA-KD. The SPE-, HD-, and KLD-based indicators are able to detect the fault but exhibit missed detections or reduced sensitivity during the fault interval. In contrast, the CCA-KD indicator provides clearer and more stable detection with minimal missed detections.

Table 10 summarizes the quantitative performance of the four indicators. The CCA-SPE method shows limited detection capability, with an F1-score of 70.79%. The CCA-HD and CCA-KLD indicators improve detection performance, achieving F1-scores of 91.75% and 93.48%, respectively. The CCA-KD method provides the best overall performance, achieving an F1-score of 99.84% and an accuracy of 99.85%, confirming its effectiveness in detecting freezing faults.

Overall, the results from the wastewater treatment process demonstrate the effectiveness of the proposed CCA-based fault detection strategy in identifying various sensor faults, including bias, intermittent, drift, and freezing faults. While the conventional SPE-based monitoring index shows limitations in detecting weak and time-varying faults, the distribution-based indicators significantly improve detection performance. In particular, the Kantorovich distance consistently provides the highest accuracy, F1-score, and robustness across all scenarios, showing strong sensitivity to small, gradual, and intermittent changes in residual distributions. These results confirm that combining CCA modeling with distribution-based residual monitoring offers a reliable and powerful framework for early fault detection in complex environmental processes.

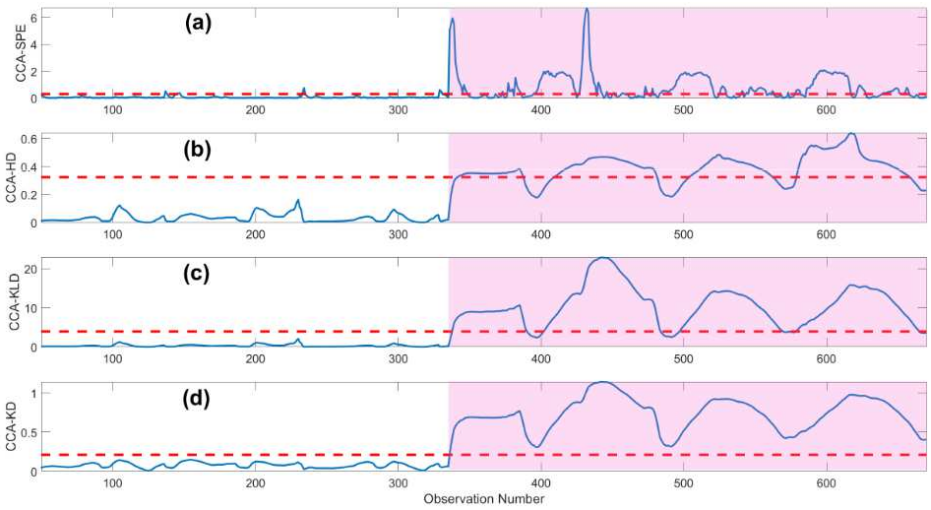


Figure 10. Freezing fault monitoring in the WWT process using CCA-based indicators: (a) SPE, (b) HD, (c) KLD, (d) KD.

Table 10. Freezing fault detection in the WWT process using CCA-based indicators (SPE, HD, KLD, KD).

Index	CCA-SPE	CCA-HD	CCA-KLD	CCA-KD
FDR	55.22	84.78	87.75	99.71
FAR	2.15	0.00	0.00	0.00
Precision	96.28	100.00	100.00	100.00
Accuracy	75.52	92.39	93.88	99.85
F1-score	70.79	91.75	93.48	99.84

Performance Comparison for Different Window Sizes To investigate the effect of the moving window length on detection performance, the freezing-fault scenario was evaluated with window sizes of 30, 40, and 50 samples. Table 11 summarizes the performance of CCA-SPE, CCA-HD, CCA-KLD, and CCA-KD for the different window sizes.

The results show that the window size primarily affects the distribution-based indicators (HD, KLD, and KD), since these methods estimate residual distributions within each window. For a window size of 30, CCA-HD and CCA-KLD exhibit few false alarms, which slightly reduces their accuracy and F1-score. In contrast, the CCA-KD method maintains strong performance with no false alarms. When the window size is increased to 40, the false alarms observed for HD and KLD disappear, resulting in improved detection performance. The CCA-KD indicator continues to deliver the best results, with higher accuracy and F1 scores. For a window size of 50, all distribution-based indicators achieve their best performance, with increased fault detection rates and improved stability. Based on these results, a window size of 50 was selected for the WWTP case study, as it provides a good compromise between detection sensitivity and robustness. Overall, the results confirm that the CCA-KD method consistently provides superior detection performance across all tested window sizes, demonstrating strong robustness to parameter selection.

5.3 Computational Complexity Analysis

The computational complexity of the proposed monitoring framework depends on two main steps: residual generation using the CCA model and the computation of the monitoring statistics within a moving window. Since the CCA model is trained offline, the online computational cost is dominated by residual projection and the evaluation of the fault indicators. The SPE statistic has the lowest computational cost, as it requires only vector–matrix operations and a quadratic form evaluation, resulting in complexity on the order of $\mathcal{O}(d^2)$ per sample, where d is the number of retained latent variables. For the distribution-based indicators, the HD and the Kullback–Leibler Distance (KLD) require estimating probability density functions within a moving window, typically using kernel density estimation. This results in a computational complexity of approximately $\mathcal{O}(W)$ to $\mathcal{O}(W^2)$ depending on the density estimation method, where W denotes the window length. The Kantorovich Distance (KD) involves solving an optimal transport problem between two empirical distributions, which is computationally more demanding, with typical complexity ranging from $\mathcal{O}(W^2)$ to $\mathcal{O}(W^3)$ depending on the implementation. However, since the window size is moderate and the computations are performed on low-dimensional residuals, the KD indicator remains practical for real-time monitoring.

Table 11. Effect of moving window size on freezing fault detection in the WWTP process using CCA-based indicators.

Size		CCA-SPE	CCA-HD	CCA-KLD	CCA-KD
30	**FDR**	55.52	74.33	79.85	98.21
	FAR	2.15	1.49	1.79	0.00
	Precision	96.28	98.03	97.81	100.00
	Accuracy	75.52	86.41	89.70	99.11
	F1-score	70.79	84.72	88.25	98.98
40	**FDR**	55.52	78.70	85.27	99.45
	FAR	2.15	0.00	0.00	0.00
	Precision	96.28	100.00	100.00	100.00
	Accuracy	75.52	89.35	92.63	99.72
	F1-score	70.79	88.08	92.04	99.69
50	**FDR**	55.22	84.78	87.75	99.71
	FAR	2.15	0.00	0.00	0.00
	Precision	96.28	100.00	100.00	100.00
	Accuracy	75.52	92.39	93.88	99.85
	F1-score	70.79	91.75	93.48	99.84

Overall, while SPE provides the lowest computational cost, HD and KLD offer improved sensitivity with moderate additional cost, and KD provides the highest detection performance at the expense of slightly increased computational effort, which remains acceptable for most industrial monitoring applications. In practical chemical and wastewater treatment processes, where sampling intervals are typically on the order of seconds or minutes, the computational time required for the proposed monitoring indices is negligible relative to the process dynamics, making the approach suitable for real-time implementation.

In summary, the results demonstrate that the distribution-based fault indicators HD, KLD, and KD significantly improve the monitoring capability of the CCA framework compared with the conventional SPE statistic, as they evaluate residual distributions within a moving-window scheme and are more sensitive to subtle changes. Among the considered indicators, the CCA-KD strategy consistently provided the best detection performance across all fault scenarios in both the Williams–Otto reactor and the wastewater treatment plant case studies. Furthermore, the analysis of different window sizes showed that smaller windows may introduce false alarms, while larger windows improve detection stability, with a window size of 50 providing the best overall performance; notably, the KD-based indicator remained the most robust across all tested configurations.

6 Conclusion

This paper presented a Canonical Correlation Analysis (CCA)-based fault detection framework enhanced with distribution-based residual monitoring using Hellinger Distance (HD), Kullback–Leibler Distance (KLD), and Kantorovich Distance (KD). The proposed approach combines latent-variable modeling with statistical distance measures to improve sensitivity to distributional changes in residuals, particularly under weak, gradual, and intermittent fault conditions. A key advantage of the proposed framework is that model training requires only fault-free data, without the need for labeled fault samples. This semi-supervised characteristic makes the method practical for real industrial and environmental systems, where fault data are often scarce, incomplete, or difficult to obtain. Detection thresholds for the distribution-based indicators were determined using a nonparametric kernel density estimation (KDE) approach, which avoids restrictive Gaussian assumptions and enables reliable threshold selection directly from normal operating data, similarly to nonparametric SPE monitoring. This improves robustness when residuals exhibit non-Gaussian or time-varying behavior. The effectiveness of the proposed method was evaluated using two benchmark processes: the Williams–Otto reactor and a wastewater treatment plant (BSM1). Several representative fault scenarios, including bias, intermittent, drift, and freezing faults, were considered. Experimental results showed that distribution-based indicators significantly improve detection performance compared with conventional SPE monitoring. Among the tested indicators, the KD-based method consistently provided the best performance in terms of detection accuracy, robustness, and sensitivity to small or time-varying faults. In addition, the influence of moving window size on detection performance was investigated. The results demonstrated that appropriate window selection improves stability and detection reliability, while the KD-based indicator remained robust across different window sizes. Overall, the results confirm that integrating CCA modeling with distribution-based residual analysis provides an effective, reliable, and practical framework for early fault detection in complex industrial and environmental processes.

Future work will investigate extensions of the proposed framework using nonlinear and kernel-based CCA as well as deep

latent variable models to better capture complex nonlinear relationships in process data. In addition, adaptive and time-varying thresholding strategies will be explored to further improve detection robustness under changing operating conditions and nonstationary environments.

7 Conflict-of-Interest Statement

No funding was received for conducting this study.

Data Availability

The datasets generated during and/or analyzed during the current study are available in Copp J B. The COST Simulation Benchmark: Description and Simulator Manual: Office for Official Publications of the European Community. Luxembourg: ISBN 92-894-1658-0; 2002.
https://iwa-mia.org/benchmarking/#BSM1

Funding Declaration

Funding: No Funding

References

1. Harrou, F., Sun, Y., Hering, A. S., Madakyaru, M. & Dairi, A. *Statistical process monitoring using advanced data-driven and deep learning approaches: theory and practical applications* (Elsevier, 2020).
2. Melo, A., Câmara, M. M. & Pinto, J. C. Data-driven process monitoring and fault diagnosis: A comprehensive survey. *Processes* **12**, 251 (2024).
3. Tang, S., Yuan, S. & Zhu, Y. Deep learning-based intelligent fault diagnosis methods toward rotating machinery. *Ieee Access* **8**, 9335–9346 (2019).
4. Yu, J. & Zhang, Y. Challenges and opportunities of deep learning-based process fault detection and diagnosis: a review. *Neural Comput. Appl.* **35**, 211–252 (2023).
5. Chang, S. I. & Ghafariasl, P. A review of artificial intelligence impacting statistical process monitoring and future directions. *arXiv preprint arXiv:2503.01858* (2025).
6. Montgomery, D. C. *Introduction to statistical quality control* (John wiley and sons, 2020).
7. Harrou, F. & Nounou, M. N. Monitoring linear antenna arrays using an exponentially weighted moving average-based fault detection scheme. *Syst. Sci. & Control. Eng. An Open Access J.* **2**, 433–443 (2014).
8. Harrou, F., Fillatre, L. & Nikiforov, I. Anomaly detection/detectability for a linear model with a bounded nuisance parameter. *Annu. Rev. Control.* **38**, 32–44 (2014).
9. Yin, S., Ding, S. X., Xie, X. & Luo, H. A review on basic data-driven approaches for industrial process monitoring. *IEEE Transactions on Ind. electronics* **61**, 6418–6428 (2014).
10. Ge, Z. Review on data-driven modeling and monitoring for plant-wide industrial processes. *Chemom. Intell. Lab. Syst.* **171**, 16–25 (2017).
11. Qin, S. J. Survey on data-driven industrial process monitoring and diagnosis. *Annu. reviews control* **36**, 220–234 (2012).
12. Cheng, T., Dairi, A., Harrou, F., Sun, Y. & Leiknes, T. Monitoring influent conditions of wastewater treatment plants by nonlinear data-based techniques. *IEEE Access* **7**, 108827–108837 (2019).
13. Taqvi, S. A. A. *et al.* A review on data-driven learning approaches for fault detection and diagnosis in chemical processes. *ChemBioEng Rev.* **8**, 239–259 (2021).
14. MacGregor, J. F. & Kourti, T. Statistical process control of multivariate processes. *Control. engineering practice* **3**, 403–414 (1995).
15. Kourti, T. Process analysis and abnormal situation detection: from theory to practice. *IEEE control systems magazine* **22**, 10–25 (2002).
16. Harrou, F., Kini, K. R., Madakyaru, M. & Sun, Y. Anomaly detection in photovoltaic systems using improved independent component analysis. *IEEE Access* (2025).
17. Russell, E. L., Chiang, L. H. & Braatz, R. D. Fault detection in industrial processes using canonical variate analysis and dynamic principal component analysis. *Chemom. intelligent laboratory systems* **51**, 81–93 (2000).

18. Chen, Z., Zhang, K., Ding, S. X., Shardt, Y. A. & Hu, Z. Improved canonical correlation analysis-based fault detection methods for industrial processes. *J. Process. Control.* **41**, 26–34 (2016).

19. Chen, Z., Ding, S. X., Peng, T., Yang, C. & Gui, W. Fault detection for non-gaussian processes using generalized canonical correlation analysis and randomized algorithms. *IEEE Transactions on Ind. Electron.* **65**, 1559–1567 (2017).

20. Chen, Z. *et al.* A distributed canonical correlation analysis-based fault detection method for plant-wide process monitoring. *IEEE Transactions on Ind. Informatics* **15**, 2710–2720 (2019).

21. Meng, S., Tong, C., Lan, T. & Yu, H. Canonical correlation analysis-based explicit relation discovery for statistical process monitoring. *J. Frankl. Inst.* **357**, 5004–5018 (2020).

22. Pilario, K. E. & Cao, Y. Process incipient fault detection using canonical variate analysis. In *2017 23rd International Conference on Automation and Computing (ICAC)*, 1–6 (IEEE, 2017).

23. Liu, C., Yang, Z., Xiang, G. & Yu, Y. A statistical feature-based anomaly detection method for pfc using canonical correlation analysis. *IEEE Transactions on Instrumentation Meas.* **71**, 1–11 (2022).

24. Gao, L., Li, D., Yao, L. & Gao, Y. Sensor drift fault diagnosis for chiller system using deep recurrent canonical correlation analysis and k-nearest neighbor classifier. *ISA transactions* **122**, 232–246 (2022).

25. Song, B. *et al.* A fault-targeted gated recurrent unit-canonical correlation analysis method for incipient fault detection. *IEEE Transactions on Ind. Informatics* **20**, 8739–8748 (2024).

26. Chen, Z., Ding, S. X., Zhang, K., Li, Z. & Hu, Z. Canonical correlation analysis-based fault detection methods with application to alumina evaporation process. *Control. Eng. Pract.* **46**, 51–58 (2016).

27. Chen, Z., Ding, S. X., Peng, T., Yang, C. & Gui, W. Fault detection for non-gaussian processes using generalized canonical correlation analysis and randomized algorithms. *IEEE Transactions on Ind. Electron.* **65**, 1559–1567 (2017).

28. Kourti, T. & MacGregor, J. F. Process analysis, monitoring and diagnosis, using multivariate projection methods. *Chemom. intelligent laboratory systems* **28**, 3–21 (1995).

29. Pilario, K. E. S. & Cao, Y. Canonical variate dissimilarity analysis for process incipient fault detection. *IEEE Transactions on Ind. Informatics* **14**, 5308–5315 (2018).

30. Basseville, M. Divergence measures for statistical data processing—an annotated bibliography. *Signal Process.* **93**, 621–633 (2013).

31. Ditzler, G. & Polikar, R. Hellinger distance based drift detection for nonstationary environments. In *2011 IEEE symposium on computational intelligence in dynamic and uncertain environments (CIDUE)*, 41–48 (IEEE, 2011).

32. Li, C., Huang, B. & Qian, F. Hellinger distance based probability distribution approach to performance monitoring of nonlinear control systems. *Chin. J. Chem. Eng.* **23**, 1945–1950 (2015).

33. Kailath, T. The divergence and bhattacharyya distance measures in signal selection. *IEEE transactions on communication technology* **15**, 52–60 (1967).

34. González, D. & Hayet, J. Fast human detection in rgb-d images with progressive svm-classification. In *Pacific-Rim Symposium on Image and Video Technology*, 337–348 (Springer, 2013).

35. Cieslak, D. & Chawla, N. A framework for monitoring classifiers' performance: when and why failure occurs. *Knowl. Inf. Syst.* **18**, 83–108 (2009).

36. Tajer, J., Makke, A., Salem, O. & Mehaoua, A. A comparison between divergence measures for network anomaly detection. In *7th International Conference on Network and Service Management*, 1–5 (IEEE, 2011).

37. Rao, C. R. A review of canonical coordinates and an alternative to correspondence analysis using hellinger distance. *Q@UMLAUT@uestiió* **19**, 23–63 (1995).

38. Yamanishi, K., Takeuchi, J.-I., Williams, G. & Milne, P. On-line unsupervised outlier detection using finite mixtures with discounting learning algorithms. *Data Min. Knowl. Discov.* **8**, 275–300 (2004).

39. Harrou, F., Madakyaru, M. & Sun, Y. Improved nonlinear fault detection strategy based on the hellinger distance metric: Plug flow reactor monitoring. *Energy Build.* **143**, 149–161 (2017).

40. Harrou, F., Madakyaru, M. & Sun, Y. Nonlinear partial least squares with hellinger distance for nonlinear process monitoring. In *2016 IEEE Symposium Series on Computational Intelligence (SSCI)*, 1–6 (IEEE, 2016).

41. Ramakrishna Kini, K., Harrou, F., Madakyaru, M., Sun, Y. & Menon, M. K. Pls-based hellinger distance method for fault detection in chemical engineering systems. *Eng. Res. Express* **6**, 035007 (2024).

42. Wang, Q., Peng, B., Xie, P. & Cheng, C. A novel data-driven fault detection method based on stable kernel representation for dynamic systems. *sensors* **23**, 5891 (2023).

43. Liese, F. & Miescke, K.-J. Statistical decision theory. In *Statistical Decision Theory: Estimation, Testing, and Selection*, 1–52 (Springer, 2008).

44. Coetzee, F. M. Correcting the kullback–leibler distance for feature selection. *Pattern Recognit. Lett.* **26**, 1675–1683 (2005).

45. Zeng, J., Kruger, U., Geluk, J., Wang, X. & Xie, L. Detecting abnormal situations using the kullback–leibler divergence. *Automatica* **50**, 2777–2786 (2014).

46. Chung, A. C., Wells III, W. M., Norbash, A. & Grimson, W. E. L. Multi-modal image registration by minimising kullback-leibler distance. In *International Conference on Medical Image Computing and Computer-Assisted Intervention*, 525–532 (Springer, 2002).

47. Anderson, A. & Haas, H. Kullback-leibler divergence (kld) based anomaly detection and monotonic sequence analysis. In *2011 IEEE Vehicular Technology Conference (VTC Fall)*, 1–5 (IEEE, 2011).

48. Harrou, F., Sun, Y. & Madakyaru, M. Kullback-leibler distance-based enhanced detection of incipient anomalies. *J. Loss Prev. Process. Ind.* **44**, 73–87 (2016).

49. Tang, Y. *et al.* Incipient fault detection based on double kullback–leibler divergence kldattw improved by a self-attention mechanism. *Reliab. Eng. & Syst. Saf.* **264**, 111247 (2025).

50. Zeroual, A., Harrou, F., Sun, Y. & Messai, N. Integrating model-based observer and kullback–leibler metric for estimating and detecting road traffic congestion. *IEEE Sensors J.* **18**, 8605–8616 (2018).

51. Kullback, S. & Leibler, R. A. On information and sufficiency. *Annals Math. Stat.* **22**, 79–86 (1951).

52. Kammammettu, S. & Li, Z. Change point and fault detection using kantorovich distance. *J. Process. Control.* **80**, 41–59 (2019).

53. Li, D. & Martínez, S. High-confidence attack detection via wasserstein-metric computations. *IEEE Control. Syst. Lett.* **5**, 379–384 (2020).

54. Lu, C., Zeng, J., Luo, S. & Cai, J. Detection and isolation of incipiently developing fault using wasserstein distance. *Processes* **10**, 1081 (2022).

55. Kini, K. R., Harrou, F., Madakyaru, M. & Sun, Y. Enhancing fault detection in wastewater treatment plants: a multi-scale principal component analysis approach with the kantorovich distance. *Environ. Sci. Water Res. & Technol.* **11**, 1215–1232 (2025).

56. Yao, Z., Jiang, Q. & Gu, X. Distributed process monitoring based on kantorovich distance-multiblock variational autoencoder and bayesian inference. *Chin. J. Chem. Eng.* **73**, 311–323 (2024).

57. Villani, C. *Optimal Transport: Old and New* (Springer, 2009).

58. Bagla, G., Patwardhan, S. C. & Bhushan, M. Development of an intelligent moving horizon estimator integrated with fault diagnosis for automated model maintenance. *J. Process. Control.* **152**, 103468 (2025).

59. Alex, J. *et al.* Benchmark simulation model no. 1 (bsm1). *Rep. by IWA Taskgroup on benchmarking control strategies for WWTPs* **1** (2008).